

JOINT INSTITUTE FOR NUCLEAR RESEARCH

Bogoliubov Laboratory of Theoretical Physics (BLTP)

FINAL REPORT ON The INTEREST PROGRAMME

Numerical Simulation of Spintronic Effects in Josephson
Nanojunctions

Supervisor

Dr. Majed Nashaat

BLTP, JINR, Dubna, Russia

Student

Anna Kalashnikova

Peoples' Friendship

University of Russia

Participation period:

February 26 - April 14

Wave 10

Dubna 2024

Abstract

If the symmetry of inversion and the symmetry with respect to time reversal is broken in ferromagnetics, a superconductor-ferromagnetic-superconductor (SFS) Josephson junction (JJ) can exhibit set of interesting features, including the change of the current-phase relation, where superconducting current turns to be linked with magnetic moment. Hence, manipulate the magnetic properties by Josephson current can be achieved. This type of SFS JJ is referred as φ_0 -Josephson junction.

This study conducts analyses of the IVC-characteristics for point contact φ_0 Josephson Junctions. We demonstrate the manifestation of ferromagnetic resonance (FMR) in the IVC and magnetization dynamics. The dynamics of the Josephson phase and magnetization within the ferromagnetic layer, is described by a system of coupled non-linear differential equations. This system of equations is obtained from the Landau-Lifshitz-Gilbert (LLG) equation and Josephson relations for current and phase difference using Resistively and capacitively shunted Josephson junctions (RCSJ) model.

Contents

1	Introduction	1
2	Model	2
3	Results	5
3.1	Rashba SOC	5
3.2	Rashba and Dresselhaus SOC	10
4	Conclusion	13
5	Acknowledgment	14

1 Introduction

The Josephson effect, predicted by Brian Josephson in 1962, is based on the tunnelling of coupled electrons through an insulating barrier [1, 2]. If a non-superconducting nano-sized material is located between two layers of a superconductor, the superconducting current will pass through this material - that is what Josephson effect means. If there is a ferromagnetic between these two superconductor layers, then it is called the anomalous Josephson effect [3]. Unlike Josephson effect which reflects the superconducting phenomenon, the anomalous effect links superconductivity and magnetism, which until recently were not combined.

First prerequisite for research into the Josephson effect was the search for weak ferromagnetic alloys to measure supercurrents via superconductor-ferromagnetic-superconductor Josephson junctions. The supercurrents in SFS junctions were firstly observed by experiments and by study of $Nb/Cu_xNi_{1-x}/Nb$ Josephson junctions. There was a transition from 0-state to π -state. The π -state is characterized by a phase shift of π in the junction's ground state. The formula, giving this state is described by $I_s(\varphi) = I_c \sin(\varphi)$, where I_c is the critical current, and φ is the phase difference between the superconductor electrodes. Recently, in Ref.[4] the authors report the observation of anomalous phase shift φ_0 in Bi_2Se_3 Josephson junctions and provide a direct measurement of the spin-orbit coupling strength. Moreover, in φ_0 junction a full magnetization reversal is demonstrated by using electric current pulse [5], while a unique possibility of controlling the magnetization dynamics via external bias current and series of specific magnetization trajectories has been reported in Ref.[6].

Moreover, π state was introduced in the first place by the prediction of Bulaevskii, in which it was proposed at the Josephson tunnel junction with magnetic impurities in the barrier at high field. Additionally they observed that a superconducting ring with a π junction could generate a spontaneous current and magnetic flux [7]. The identification of the π junction encouraged further experimental investigation, resulting in an elaborate explanation of some of the novel effects observed under different ferromagnetic alloy interlayer. Steps from 0 to π state in the system of superconducting flux junctions were investigated in different ways [8]. This lead to the development of an outlook of a complex current phase relations (CPR) as a result of studies on the π transitions.

Recent theoretical work has predicted the generation of a long-range triplet order parameter in structures with inhomogeneous magnetization or noncollinear orientations of magnetization

in different F layers. The Josephson effect in junctions between unconventional superconductors across different types of magnetic barriers has also been explored theoretically [7].

Systems exhibiting π states encompass planar SFS proximity-effect structures, tunnel junctions with magnetic insulators or magnetically active interfaces, and structures with barriers containing multiple magnetic layers.

This study will focus on the fundamental aspects of the Josephson effect in SFS junctions containing Rashba spin-orbit coupling SOC and Rashba- Dresselhaus spin orbit coupling.

2 Model

In this section, we investigate the φ_0 junction, in which the SOC provides a direct coupling between Josephson phase and magnetic moment of ferromagnetic barrier.

We consider an SFS anomalous Josephson junction with SOC [9]. The geometry of the considered φ_0 junction is shown in Fig.1. The ferromagnetic easy-axis and the gradient of the spin-orbit potential (\mathbf{n}) are directed along the z-axis. Due to the interplay between the exchange field and the SOC, the CPR of the SFS junction is given as $I = I_c \sin(\varphi - \varphi_0)$. The anomalous phase shift ϕ_0 is dependent on SOC and the geometry of the device. Taking into consideration a two dimensional SOC with momenta in the x-y plane with both Rashba and Dresselhaus contribution, the anomalous phase shift for the particular geometry considered according to [10] can be written in the following form:

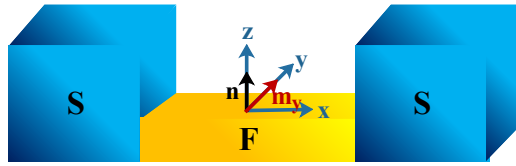


Figure 1: Geometry of the φ_0 - junction. S - superconductor, F - ferromagnet, \mathbf{n} - unit vector of the gradient of the spin-orbit potential. The Josephson current flows in the x direction.

$$\varphi_0 = r_{\beta_{SOC}}(\beta_{SOC}m_x + m_y) \quad (1)$$

where $\beta_{SOC} = \beta/\delta$ is the ratio between SOC coefficients, where β is the Dresselhaus coefficient, δ is the Rashba coefficient, $r_{\beta_{SOC}} = r(1 - \beta_{SOC}^2)$ is the SOC strength accounting for the dependence of both δ and β .

The dynamics of magnetization of the F-layer is described by the Landau-Lifshitz-Gilbert (LLG) equation. Here taking into account the expression 1 for the phase shift, the effective field according to [10] is given as:

$$\mathbf{H}_{eff} = \frac{K}{M_0} [Gr_{\beta_{soc}} \sin(\varphi - \varphi_0) (\beta_{soc} \hat{\mathbf{x}} + \hat{\mathbf{y}}) + m_z \hat{\mathbf{z}}] \quad (2)$$

where $G = E_J/(K\nu)$ is the ratio of the Josephson energy to the magnetic one where K is the anisotropic energy term, ν is the volume of the ferromagnetic layer.

$$\begin{aligned} \dot{m}_x &= \frac{\omega_F}{1 + M_s \alpha^2} \{m_z [h_y + \alpha(h_x m_z - h_z m_x)] + h_x \alpha m_y^2 - m_y (h_z + h_y \alpha m_x)\} \\ \dot{m}_y &= \frac{\omega_F}{1 + M_s \alpha^2} \{m_x [h_z + \alpha(h_y m_x - h_x m_y)] + h_y \alpha m_z^2 - m_z (h_x + h_z \alpha m_y)\} \\ \dot{m}_z &= \frac{\omega_F}{1 + M_s \alpha^2} \{m_y [h_x + \alpha(h_z m_y - h_y m_z)] + h_z \alpha m_x^2 - m_x (h_y + h_x \alpha m_z)\} \\ \dot{V} &= \frac{1}{\beta_c} [I + A \sin(\omega_R t) - \sin(\varphi - \varphi_0) - V + r_{\beta_{soc}} (\beta_{soc} \dot{m}_x + \dot{m}_y)], \quad \dot{\varphi} = V \end{aligned} \quad (3)$$

where β_c is the McCumber parameter, $m_i = M_i/M_0$ for $i = x, y, z$ is the normalized magnetization, $m_i = M_i/M_0$ for $i = x, y, z$ is the effective field normalized to K/M_s , $\omega_F = \Omega_F/\omega_c$ here the ferromagnetic resonance frequency $\Omega_f = \gamma K/M_0$ and the characteristic junction frequency $\omega_c = 2eRI_c/\hbar$ and we normalize time in unites of ω_c^{-1} , current in unites of I_c , and the voltage in unites of $I_c R$.

From the definition of β_{soc} and the parameter $r_{\beta_{soc}}$, we can disregard the Dresselhaus contribution by considering $\beta_{soc} = 0$ thus $r_{\beta_{soc}} \rightarrow r$ and only Rashba SOC is considered. Another possibility is to have similar contribution of the Rashba and Dresselhaus SOC thus $\beta_{soc} = 1$, leading to $r_{\beta_{soc}} = o$ and from expression 1 we see that this will result in the phase-shift vanishing thus decoupling the supercurrent and magnetic moment and we return to a model similar to that of the SIS junction. This is intriguing since the Rashba SOC can be controlled by a gate voltage giving the possibility of tuning β_{soc} , and hence the phase-shift and the supecurrent [11].

To solve this system and calculate the IV-characteristics, we assume a constant bias current and calculate the voltage from the Josephson relation $V(\tau) = d\theta/d\tau$. We employ a 4th-order Runge-Kutta integration scheme which conserves the magnetization magnitude in time. The dc

bias current I is normalized to the critical current I_c^0 , and the voltage $V(t)$ to $\hbar\omega_c/(2e)$. As a result, we find the temporal dependence of the voltage in the JJ at a fixed value of bias current I . Then, the current value is increased or decreased by a small amount, δI (the bias current step), to calculate the voltage at the next point of the IV-characteristics. We use the final phase and voltage achieved at the previous point of the IV-characteristics as the initial condition for the next current point. The average of the voltage $V(\tau)$ is given by $V = \frac{1}{T_f - T_i} \int_{T_i}^{T_f} V(\tau) d\tau$, where T_i and T_f determine the interval for the temporal averaging. Further details of the simulation procedure are described in Ref.[12]. The initial conditions for the magnetization components are assumed to be $m_x = 0$, $m_y = 0$ and $m_z = 1$, while for the voltage and phase we take zeros.

3 Results

3.1 Rashba SOC

In this section, we present the simulation results for solving the system of equations (3) at different model parameters. In Fig. 2 we demonstrate the effect of spin orbit coupling "r" on the IV-characteristic for φ_0 JJ. The IV-characteristic is calculated by increasing the bias current from 0 to I_{max} (here it is equal 2), then the current is decreased to 0. Since we consider underdamped case, the IVC demonstrates hysteric effect. In the first part for increasing current, the voltage is zero until $I > I_c$, then we jump to resistive state, with slope satisfy Ohm's law. Next, when the current decreases, and near ferromagnetic resonance (FMR) region ($V = \omega_J \approx \omega_F, \omega_F/2$), the IV-characteristic shows a strong nonlinear features (see upward and downward insets). The IV-curve deviates from Ohm's current-voltage characteristic, the degree of deviation depends on the value of the SOC.

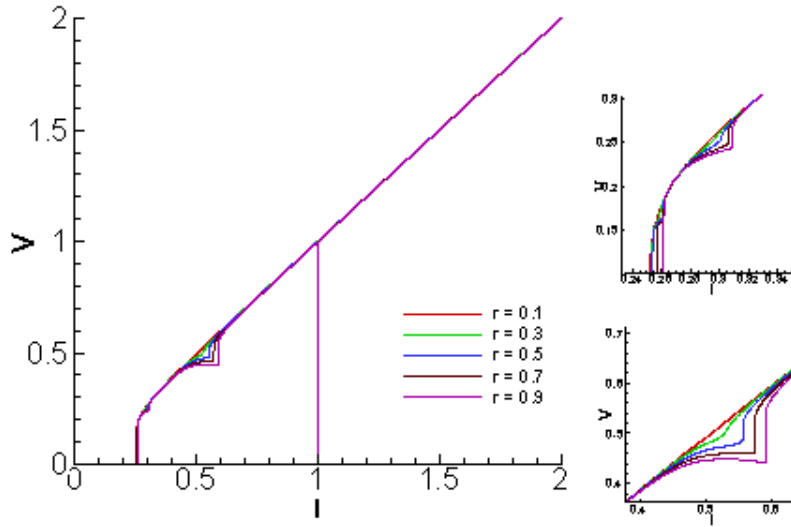


Figure 2: IV-characteristic for φ_0 JJ at different values of r with $G = 0.05$. The insets show enlarged part of the IVC at $V \approx 0.25 = \omega_F/2$, $V \approx 0.5 = \omega_F$ respectively.

On the other hand, the effect of the energy ratio of the Josephson to the magnetic one "G" on the IV-characteristic is shown in Fig. 3. By increasing the "G" value, the resonance region changes dramatically and the return current changes depending on the G value in contrast to

the case with different SOC (see inset).

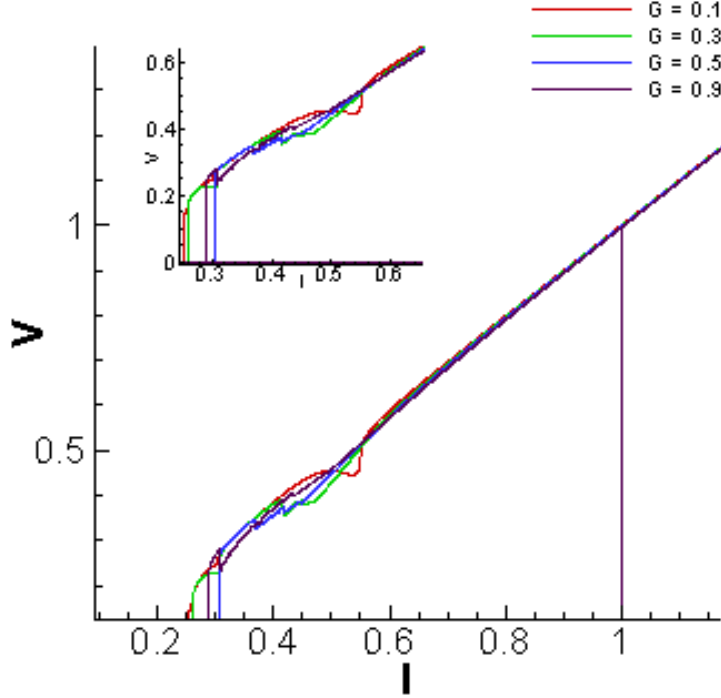


Figure 3: IV-characteristic for φ_0 JJ at different values of G with $r = 0.4$. The inset shows an enlarged part of the IVC.

In order to show the manifestation of the FMR, we plot the IVC, $m_y^{max}(I)$ and $I_s(I)$ in Fig.4 at $r = 0.7$ and $G = 0.05$. The curve for $m_y^{max}(I)$ demonstrates peaks in the resonance regions. In this regions also, the $I_s(I)$ has finite vales, indicating an increase of supercurrent tunneling. In addition to this, in the IVC resonance region, a region of negative differential resistance appears where the voltage decreases as the current increases. This is happening due to the spin orbit interaction that leads to the connection between the Josephson phase and magnetic moment dynamics in the considered Junction.

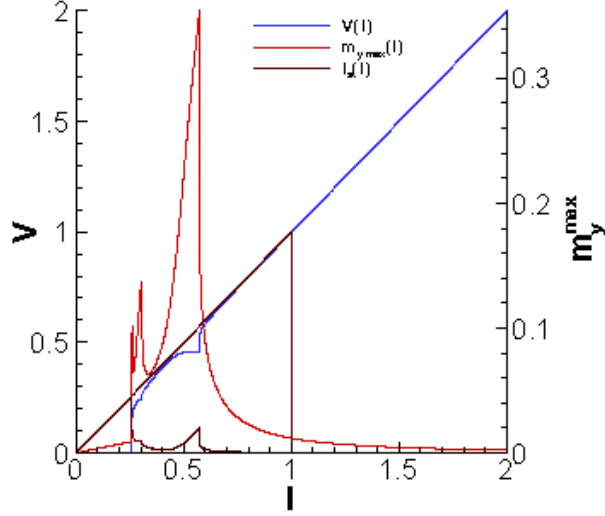


Figure 4: IV-characteristic, I_s and m_y^{max} for φ_0 JJ at $r = 0.7$ and $G = 0.05$.

Next, we record the magnetization trajectory at several regions in the IVC which is shown in Fig.4. The results are demonstrated in Fig.5 for different planes (m_x, m_y and m_z). First row of curves relates to bias current $I = 0.52$ which corresponds to the resonance peak (see Fig.4). The trajectory is represented by a circle $m_y - m_x$ plane, and a butterfly in $m_z - m_x$, and $m_y - m_z$ planes. By increasing the current, the trajectories changes see the 2nd row for $I = 0.55$. At $I=1.5$ the component of magnetic moment in z-direction is almost one. The above results presents a way to control the magnetization dynamics via external bias current I . The dynamics of magnetization is very simple here and corresponds to the rotation of the magnetic moment around different axes.

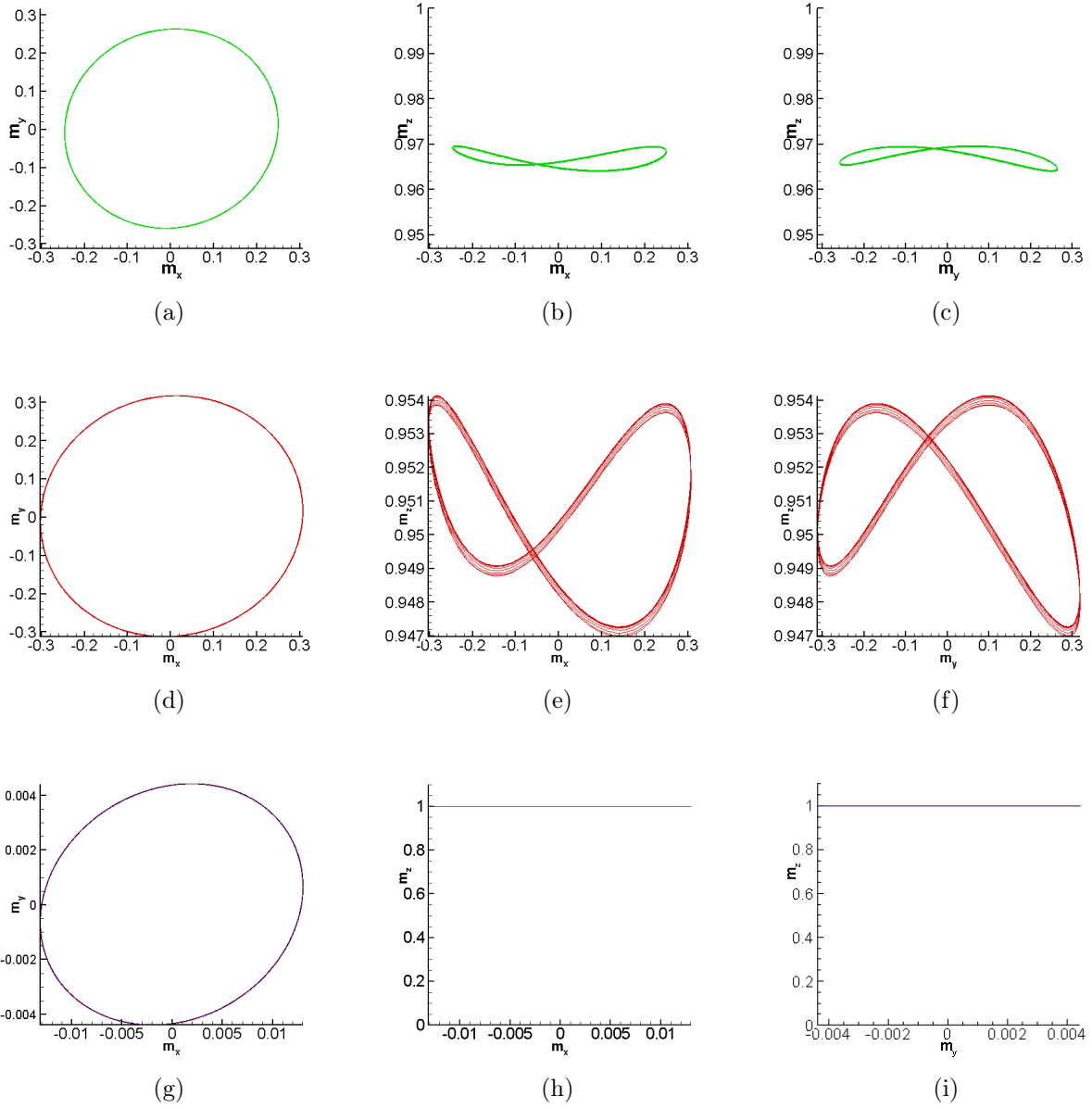


Figure 5: Magnetization trajectories in the planes $m_y - m_x$, $m_z - m_x$, and $m_z - m_y$ for $r = 0.7$ and $I = 0.52$, $I = 0.55$, $I = 1.5$

In Fig. 6 we present results of a detailed fast Fourier transform (FFT) analysis of the time dependence of the magnetization components and voltage for JJs at different biasing currents. Comparing the results presented in Fig. 6, we find that the dynamics of magnetization in this case is really determined by Josephson frequency. We also note the effect of the magnetic

oscillations on Josephson current which is manifested as a small peak in the FFT of $V(t)$ (see inset) corresponds to the second harmonic.

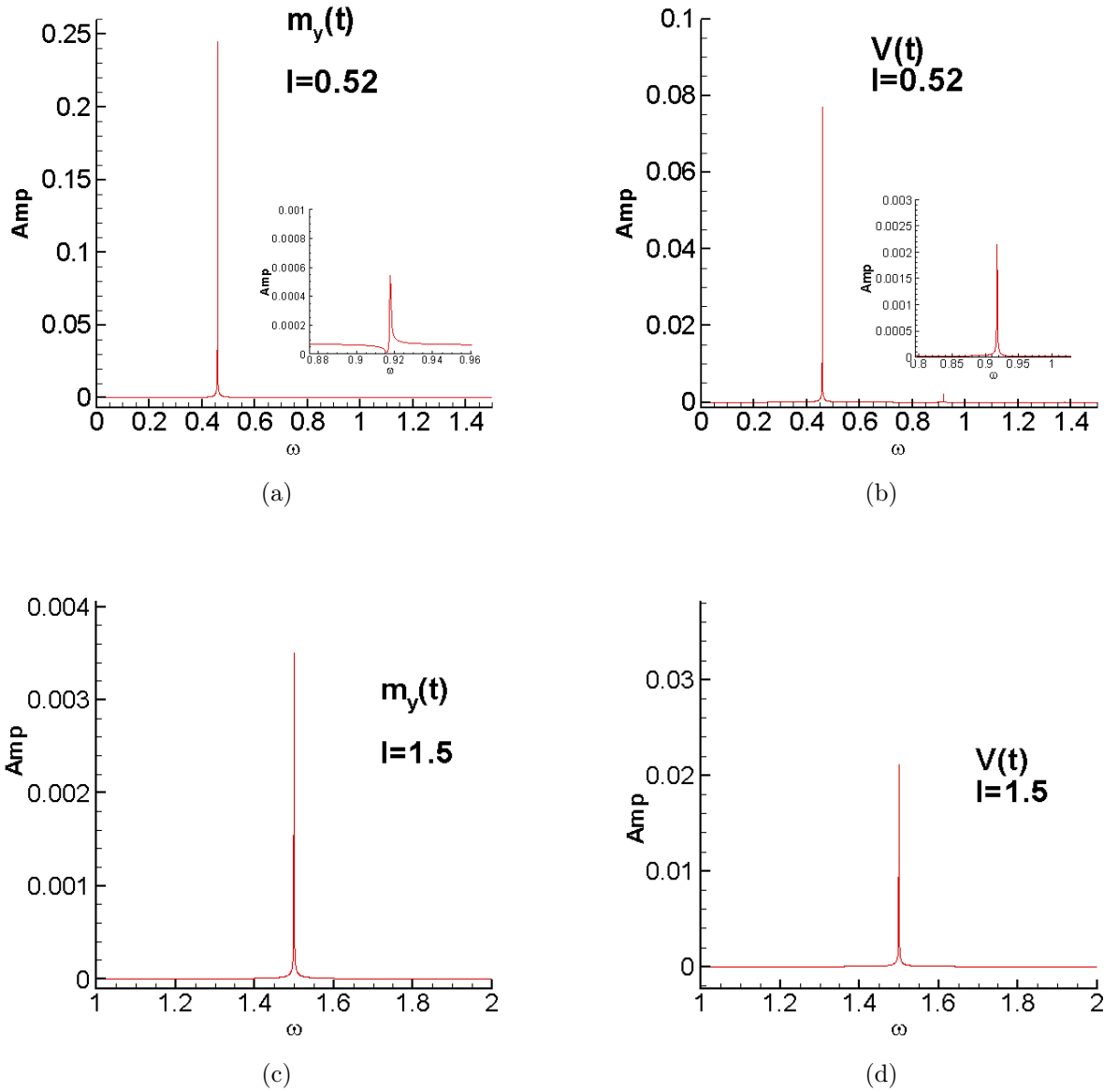


Figure 6: (a) and (b) Fast Fourier transform for magnetic moment ($m_y(t)$) and voltage voltage dynamics respectively at $I = 0.52$. (c) and (d) the same for (a,b) but for $I = 1.5$.

3.2 Rashba and Dresselhaus SOC

In this section, we present simulation results for the case with Dresselhaus spin orbit coupling ($\beta_{soc} \neq 0$). Fig. 7 shows the voltage dependence of m_x^{max} at different β_{soc} . It reflects the effect of the spin-orbit interaction on the resonance character of the Voltage and (m_x^{max}) dependence. The contribution to the Josephson current manifests itself as a deviation of the IV curve from the linear dependence in the resonance region.

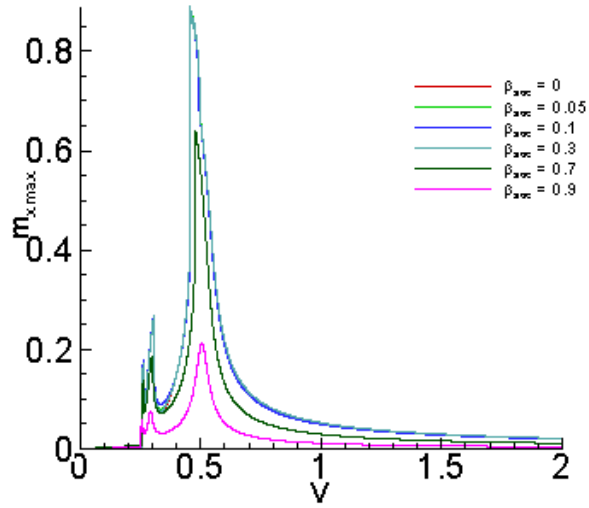


Figure 7: The voltage dependence of the maximum amplitude of m_x for different values of β_{soc} .

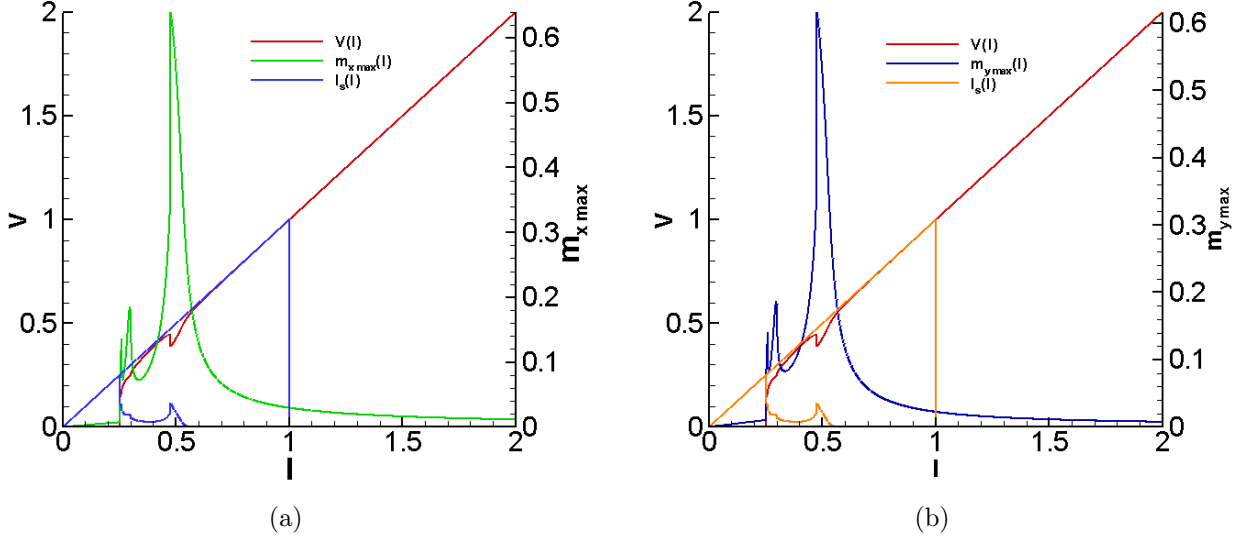


Figure 8: IV-characteristic, I_s and m_x^{max} (a), m_y^{max} (b) for $\beta_{soc} = 0.7$

Fig.8 demonstrates the manifestation of the FMR for the case with Dresselhaus SOC. We can see an increase of the magnetization amplitude m_y^{max} and m_x^{max} in the resonance region near $\omega_F = 0.5$. This resonance is also manifested in the IV-characteristics as the corresponding resonance branch. We note that due to the nonlinearity in our system, which reflects the nonlinear nature of the LLG equation, the resonance frequency decreases with an increasing in SOC or damping in the system, i.e. the resonance realized at $\omega_J < \omega_F$. So, the end of the resonance branch does not coincide with ω_F . We see also the manifestation of two FMR subharmonics corresponded to $V = \omega_F / 2$. The superconducting current which is demonstrated in this figure also reflects the FMR.

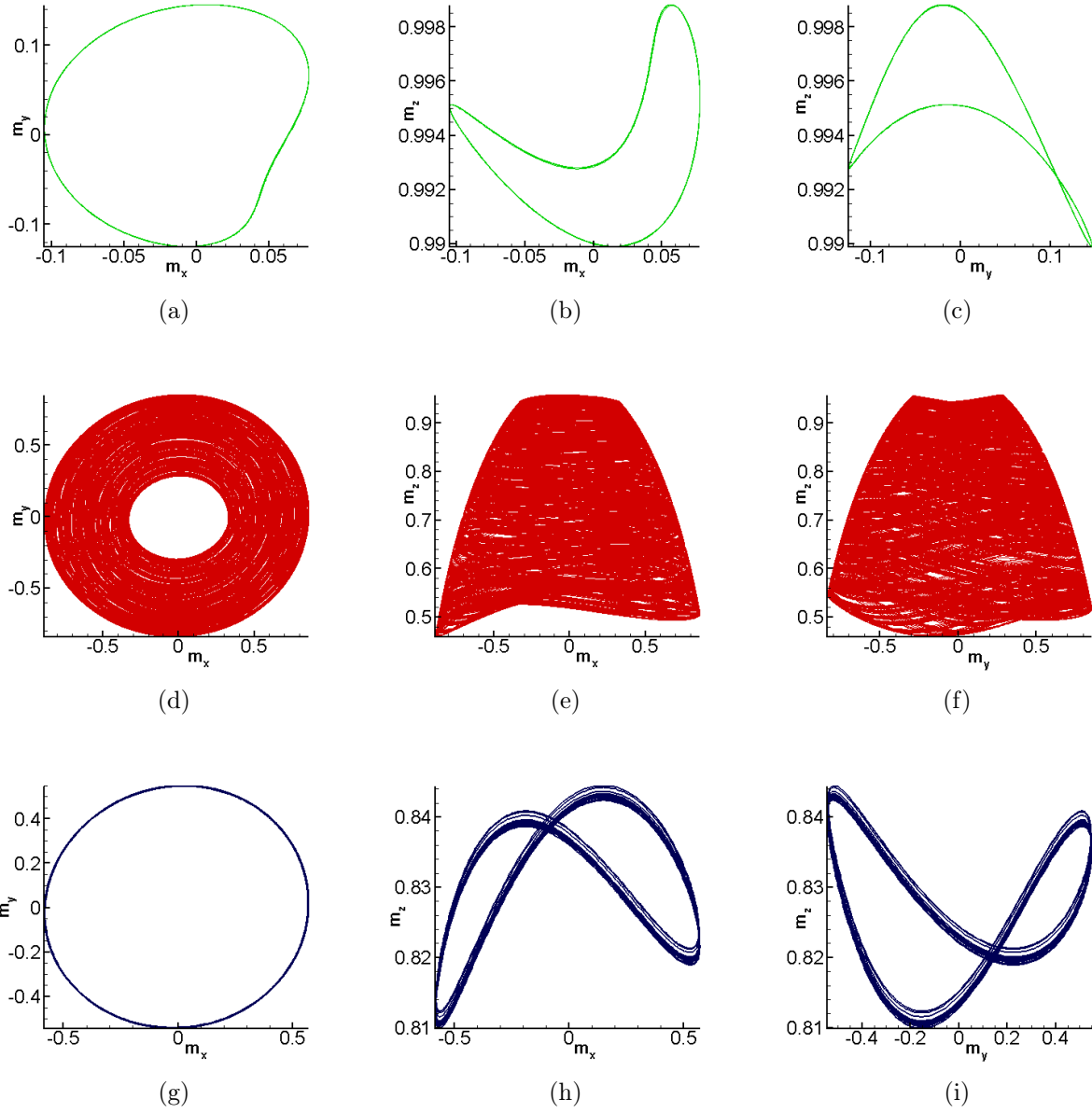


Figure 9: Magnetization trajectories in the planes $m_y - m_x$, $m_z - m_x$, and $m_z - m_y$ for $\beta_{soc} = 0.05$ and $I = 0.34$, $I = 0.47$, $I = 0.52$

The transformation of magnetization trajectory is shown in Fig.9 for different planes. Third line of curves relates to bias current $I = 0.52$ which corresponds to the resonance peak (see Fig.8).

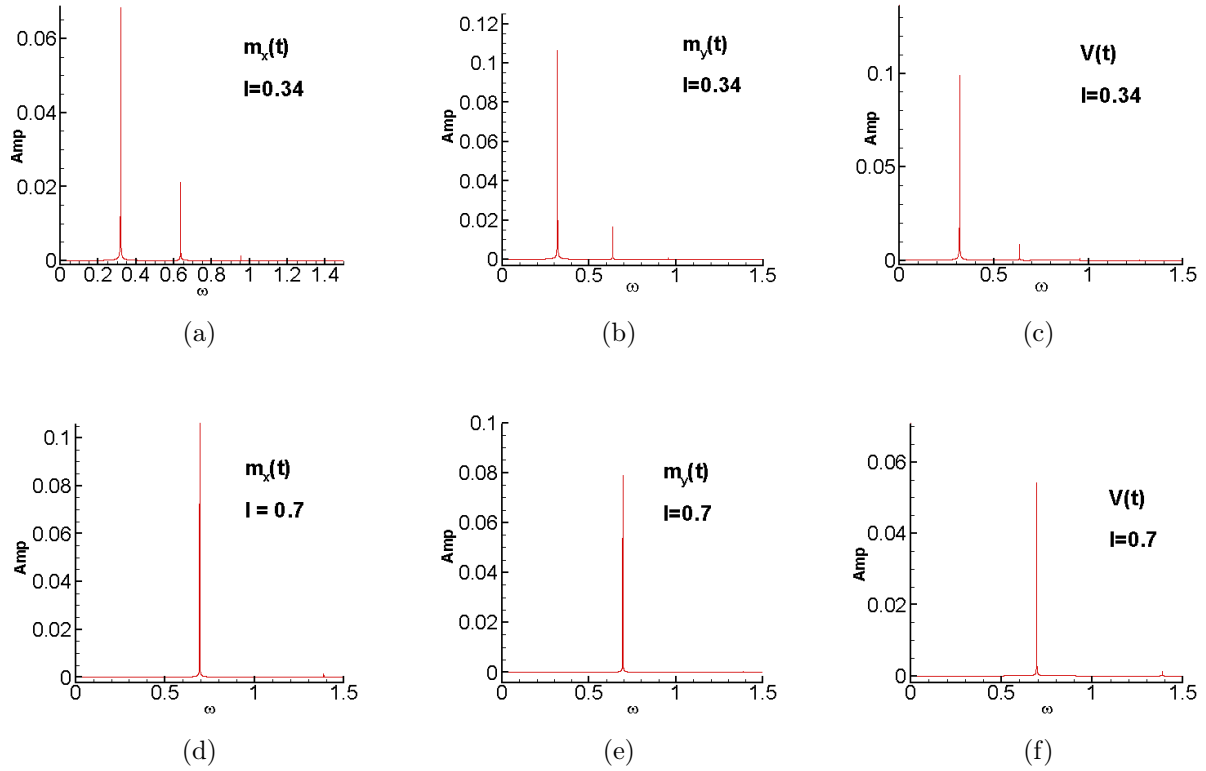


Figure 10: FFT analysis of time dependencies of (a), (d) $m_x(t)$; (b), (e) $m_y(t)$; (c), (f) $V(t)$; for $\beta_{soc} = 0.05$ and $I = 0.34$, $I = 0.7$ respectively.

In Fig. 10 we present the results of FFT analysis of the time dependence of the magnetization components and voltage for JJs with the magnetic system at $I = 0.34$ and $I = 0.7$. Comparing the results presented in Fig. 10, we find that the dynamics of magnetization in this case is determined by Josephson frequency. The existence of half harmonics in this parameter regime indicates that the excitation of magnetic dynamics happens parametrically.

4 Conclusion

In summary, we studied the phase and magnetic moment dynamics for φ_0 JJ. The dynamics of critical current and the IV characteristic can be affected by the coupling between Josephson phase and magnetization in the F-layer. We demonstrate the manifestation of ferromagnetic resonance on the current voltage characteristic and magnetization dynamics, for different type

and values of spin orbit coupling. Due to the spin orbit coupling, a nonlinear IV curve appears in the resonance regions, when the normalized voltage is close to the ferromagnetic resonance frequency. In addition to this, we demonstrate the manipulation of the magnetization trajectories by the biasing current for the proposed junction.

5 Acknowledgment

Special thanks for Prof. Shukrinov group for providing the code for the calculations.

References

- [1] B. D. Josephson. Possible new effects in superconductive tunnelling. *Physics letters*, 1(7):251–253, 1962.
- [2] K. K. Likharev. Superconducting weak links. *Reviews of Modern Physics*, 51(1):101, 1979.
- [3] A. Buzdin. Direct coupling between magnetism and superconducting current in the josephson φ 0 junction. *Physical review letters*, 101(10):107005, 2008.
- [4] A. Assouline, C. Feuillet-Palma, N. Bergeal, T. Zhang, A.Mottaghizadeh, A. Zimmers, E. Lhuillier, M. Eddrief M. Marangolo, P. Atkinson, M. Aprili, and H. Aubin. *âNat. Commun.*, 10(1):126, 2019.
- [5] K. Sengupta Yu. M. Shukrinov, I. R. Rahmonov and A. Buzdin. Magnetization reversal by superconducting current in φ josephson junctions. *Applied Physics Letters*, 110(18), 2017.
- [6] Yu. M. Shukrinov, I. R. Rahmonov, and K. Sengupta. Ferromagnetic resonance and magnetic precessions in φ 0 junctions. *Physical Review B*, 99(22):224513, 2019.
- [7] A. A. Golubov, M. Yu. Kupriyanov, and E. IlâIchev. The current-phase relation in josephson junctions. *Reviews of modern physics*, 76(2):411, 2004.
- [8] Yu. M. Shukrinov. Anomalous josephson effect. *Physics-Uspekhi*, 65(4):317, 2022.
- [9] F. Konschelle and A. Buzdin. Magnetic moment manipulation by a josephson current. *Physical Review Letters*, 102(1):017001, 2009.

- [10] C. Guarcello and F. S. Bergeret. Cryogenic memory element based on an anomalous josephson junction. *Physical Review Applied*, 13(3):034012, 2020.
- [11] F. Dettwiler, J. Fu, et al. Stretchable persistent spin helices in gaas quantum wells. *Physical Review X*, 7(3):031010, 2017.
- [12] A. E. M. Nashaat, Botha, and Yu. M. Shukrinov. Devil's staircases in the iv characteristics of superconductor/ferromagnet/superconductor josephson junctions. *Physical Review B*, 97(22):224514, 2018.